Polymer 50 (2009) 1288–1296

Contents lists available at ScienceDirect

Polymer

journal homepage: www.elsevier.com/locate/polymer

Suppression of crystallization in a plastic crystal electrolyte (SN/$LiClO_4$) by a polymeric additive (polyethylene oxide) for battery applications

Ruijuan Yue [a,b], Yanhua Niu [a], Zhigang Wang [a,*], Jack F. Douglas [c], Xingqi Zhu [d], Erqiang Chen [d]

[a] CAS Key Laboratory of Engineering Plastics, Beijing National Laboratory for Molecular Sciences, Institute of Chemistry, Chinese Academy of Sciences, 100190 Beijing, PR China
[b] Graduate School of Chinese Academy of Sciences, 100049 Beijing, PR China
[c] Polymers Division, National Institute of Standards and Technology, Gaithersburg, MD 20899, United States
[d] Beijing National Laboratory for Molecular Sciences, Key Laboratory of Polymer Chemistry and Physics of Ministry of Education, College of Chemistry and Molecular Engineering, Peking University, 100871 Beijing, PR China

ARTICLE INFO

Article history:
Received 1 December 2008
Received in revised form
5 January 2009
Accepted 10 January 2009
Available online 15 January 2009

Keywords:
Crystallization
Plastic crystal electrolyte
Polyethylene oxide

ABSTRACT

A basic problem with many promising solid electrolyte materials for battery applications is that crystallization in these materials at room temperature makes ionic mobilities plummet, thus compromising battery function. In the present work, we consider the use of a polymer additive (polyethylene oxide, PEO) to *inhibit* the crystallization of a promising battery electrolyte material, the organic crystal forming molecule succinonitrile (SN) mixed with a salt ($LiClO_4$). While SN spherulite formation still occurs at low PEO concentrations, the SN spherulites become progressively irregular and smaller with an increasing PEO concentration until a 'critical' PEO concentration (20% molar fraction PEO) is reached where SN crystallization is *no longer observable* by optical microscopy at room temperature. Increasing the PEO concentration further to 70% (molar fraction PEO) leads to a high PEO concentration regime where PEO spherulites become readily apparent by optical microscopy. Additional diffraction and thermodynamic measurements establish the predominantly amorphous nature of our electrolyte–polymer mixtures at intermediate PEO concentrations (20–60% molar fraction PEO) and electrical conductivity measurements confirm that these complex mixtures exhibit the phenomenology of glass-forming liquids. Importantly, the intermediate PEO concentration electrolyte–polymer mixtures retain a relatively high conductivity at room temperature in comparison to the semicrystalline materials that are obtained at low and high PEO concentrations. We have thus demonstrated an effective strategy for creating highly conductive and stable conductive polymer–electrolyte materials at room temperature that are promising for battery applications.

1. Introduction

Interest in plastic crystal electrolytes has recently been revived after some ionic [1–5] and molecular plastic crystals [6,7] have been shown to exhibit significant conductivity and good mechanical properties at room temperature. From a practical standpoint, plastic crystal electrolyte mixtures are attractive technologically in connection with the development of rechargeable lithium batteries [1,7].

Up to the present, succinonitrile (SN) is the only molecular plastic crystal material in this class that has the physical characteristics suitable for lithium battery production. This is mainly due to its formation of a plastic crystal phase in the convenient temperature range between 233 K and 331 K. SN materials thus provide a natural starting point for investigations in this area. The plastic crystal is rendered a conducting electrolyte by mixing with a salt, but no particular electrolyte has been demonstrated to be of particular advantage when mixed with SN. This aspect of plastic crystal electrolytes is still under investigation. Nonetheless, it has been found that promising properties for battery applications can be obtained by doping SN with lithium salts, such as lithium bis-tri-fluoromethane-sulfonimide (LiTFSI), lithium trifluoromethanesulfonate ($LiCF_3SO_3$) and lithium tetrafluoroborate ($LiBF_4$) [6], and we accordingly restrict our attention to Li salts mixed with SN in our investigation.

The mechanical properties of plastic crystal electrolytes are often unsuitable or inconvenient for the intended applications of these materials and efforts have been made to enhance the mechanical strength of these materials in particular by using

* Corresponding author. Tel./fax: +86 10 62558172.
E-mail address: zgwang@iccas.ac.cn (Z. Wang).

0032-3861/$ – see front matter © 2009 Elsevier Ltd. All rights reserved.
doi:10.1016/j.polymer.2009.01.022

various additives. Polymers are a natural choice for such additives, but traditional polymer–electrolytes, formed by solvent-free polymers (such as polyethylene oxide; PEO) and metal salts, have shown disadvantages, such as a propensity for the polymer to crystallize and a tendency for the salt to exhibit a low degree of dissociation within the polymer filled medium. These technical obstacles have impeded the practical development of lithium batteries based on these mixtures [8–11]. Previous attempts at creating such plastic crystal electrolyte–polymer mixtures have been frustrated by a trade-off in properties. For example, Abu-Lebdeh et al. [12] added a small amount of a non-aqueous ionic liquid (composed of imidazole and bis(tri-fluoromethylsulfonyl)imide) to a SN electrolyte to obtain a material having a high conductivity, but when they added a small concentration of polyacrylonitrile (PAN) to this conductive mixture the conductivity decreased dramatically. Abu-Lebdeh et al. attributed the decrease of conductivity to an unspecified 'interaction' between polymer chains and the plastic crystal phase and did not consider the impact of mixing these materials on the specific crystallization morphology [12]. Fan et al. have studied SN/LiTFSI electrolytes with polyethylene oxide (PEO) as the polymer additive, and found that the PEO/SN/LiTFSI (70/25/5) electrolyte mixtures had a relatively high ionic conductivity and improved mechanical properties [13]. In addition, poly(vinylidene fluoride-*co*-hexafluoropropylene) (PVDF-*co*-HFP) has also been used as a polymer additive in developing electrolytes for battery applications [14]. These observations together suggest a promising strategy of obtaining electrolyte materials having both good mechanical and electrical properties, provided the tendency towards polymer or electrolyte material crystallization can be brought under better control. A basic question considered by the present work is whether it is possible to overcome this difficulty through an optimized choice of polymer additive and its concentration for a model plastic crystal electrolyte.

We investigate plastic crystal electrolytes consisting of succinonitrile (SN) and a Li salt having a relatively low hygroscopic character (lithium perchlorate, $LiClO_4$) and PEO is chosen as the polymeric additive due to its widespread availability, low cost and relative ease of processing. Our approach is based on the hypothesis that it might be possible to control crystallization in the SN plastic crystal electrolyte by introducing yet another crystallizing species (such as PEO) that would *interfere with the crystallization* of the plastic crystal electrolyte through the disorder created by the PEO crystallization. The optimal conditions for achieving this frustration effect were unclear at the onset of our investigation so we thoroughly investigated the morphology, phase behavior and ionic conductivity of these PEO–electrolyte mixtures over a wide range of temperatures and polymer compositions. The experimental methods employed were also diverse, including polarized optical microscopy (POM) and wide-angle X-ray diffraction (WAXD) to characterize large and small scale structures, differential scanning calorimetry (DSC), and conductivity measurements. We find that the strategy of using polymer additives to frustrate the crystallization of another species is indeed effective for the plastic electrolyte–polymer mixtures. In particular, we obtain relatively uniform glassy materials at intermediate PEO concentrations that are stable against large-scale crystallization and that exhibit high conductivities promising for lithium battery applications.

2. Experimental

Succinonitrile (>99% purity by mass) was supplied by Tokyo Chemical Industry Co. [15], $LiClO_4$ (99% purity by mass) was supplied by Alfa Aesar Co. and PEO (relative number and weight average molecular masses, $M_n = 92{,}000$ and $M_w = 166{,}000$, respectively, by gel permeation chromatography) was provided by Changchun Dadi Fine Chemical Co. $LiClO_4$ and PEO were respectively dried in vacuum oven at 120 °C for 72 h and at 50 °C for 48 h before use. Acetone was supplied by the Beijing Chemical Plant and was dried over anhydrous $CaSO_4$ and then distilled before use.

PEO/SN/$LiClO_4$ electrolytes having a range of compositions (molar ratio) were prepared by solution blending method. Due to hygroscopic nature of this class of materials, all handling, balancing and mixing processes were carried out in glove box filled with argon gas. PEO, SN and $LiClO_4$ were dissolved in dry acetone and these mixtures were continuously stirred at room temperature for 12 h and at 50 °C for 12 h until the mixture appeared homogeneous. The mixtures were then treated in a N_2-flushed glass box for 24 h to evaporate acetone. Finally, the PEO/SN/$LiClO_4$ samples obtained from this procedure were dried in vacuum oven at 30 °C for 2 d before further measurements. In the PEO/SN/$LiClO_4$ samples, the molar percent of $LiClO_4$ was fixed at 5%, and the total molar percent of both PEO and SN was 95% (all concentrations below are in molar percent unless otherwise indicated). PEO/SN/$LiClO_4$ 0/95/5 sample was prepared by adding $LiClO_4$ directly into the molten SN. The compositions of the PEO/SN/$LiClO_4$ samples by molar ratio were designated: 0/95/5, 10/85/5, 20/75/5, 30/65/5, 40/55/5, 50/45/5, 60/35/5, 70/25/5, 75/20/5, 85/10/5 and 95/0/5.

Pure plastic crystal SN is a waxy solid at room temperature. The flexibility of samples as a solid did not change appreciably with addition of 5% $LiClO_4$ or by the additions of 5% $LiClO_4$, 10% PEO to SN. Thus, the samples of PEO/SN/$LiClO_4$ 0/95/5 and 10/85/5 had almost the same deformability as SN at room temperature. However, increasing the PEO concentration from 20% to 70% (PEO/SN/$LiClO_4$ samples: 20/75/5, 30/65/5, 40/55/5, 50/45/5, 60/35/5 and 70/25/5) gave rise to an apparently amorphous glassy material having a progressively large viscosity with an increasing PEO concentration or upon lowering the temperature. The material became 'gel-like' in consistency (rheology measurements on these materials are considered below) at the highest PEO concentration in this range. Specifically, when the PEO concentration increased from 75% to 85%, corresponding to the samples of PEO/SN/$LiClO_4$ 75/20/5 and 85/10/5, the polymer–electrolyte mixtures became firm solids at room temperature with no apparent fluidity. Increasing the PEO concentration further to 95% (the sample of PEO/SN/$LiClO_4$ 95/0/5), led to the formation of a rigid material due to a high PEO crystallinity, a phenomenon commonly encountered in PEO–electrolyte materials [16,17].

The ionic conductivities of the SN, SN/$LiClO_4$ and PEO/SN/$LiClO_4$ samples were measured by using AC impedance device (HIOKI LCR 3520 HI TESTER, made in Japan) at 1 kHz. Each sample was placed in 1 mm thick Teflon spacer ring before being compressed between two stainless steel electrodes and the samples were then sealed in homemade test cell where the area of the electrodes was $\approx 0.5\ cm^2$. The test cell was placed into oven coupled with a temperature controller. The conductivity data of each sample were recorded for every 3–5 °C over a range from room temperature to 80 °C. For each temperature, a waiting period of at least 30 min was made before the data were recorded. The standard relative uncertainty of the conductivity measurements for each temperature was less than 5%.

A polarized optical microscope (Leica DM LP-MP30, Wetzlar, Germany) equipped with a charged coupled device (CCD) camera (Pixera Pro 150 ES, San Jose, USA) was used for large-scale morphological observations on our PEO/SN/$LiClO_4$ samples, where all optical micrographs were taken with crossed-polarized light. The samples were placed between two cover glasses and then they were pressed into films with thicknesses of 15–20 μm. The standard relative uncertainty of the film thickness was estimated to be less than 3%. The PEO/SN/$LiClO_4$ samples with % PEO molar concentration of 0%, 10%, 20% and 95% and the PEO sample could not be pressed into films at room temperature and so these samples were

pressed into films at 80 °C and then were quickly cooled to room temperature for observation.

Thermal properties and the ordering transition temperatures of the PEO/SN/$LiClO_4$ samples were measured on a Perkin–Elmer Diamond differential scanning calorimetry (DSC) instrument. Specimens of about 5 mg were hermetically sealed in aluminum pans in an Ar-filled glove box. The DSC scanning procedure for each sample was as follows: first, the sample was heated from −100 °C to 80 °C at a rate of 10 °C min^{-1} to detect phase transitions. The sample was then held at 80 °C for 5 min to largely 'erase' the former thermal history, and finally the sample was cooled from 80 °C to −100 °C at a rate of 10 °C min^{-1} to ascertain potential hysteresis and the reproducibility of phase transition temperature determinations where the DSC scanning was performed under a helium atmosphere. Indium was used for calibrating the temperature and enthalpy determinations.

Two-dimensional wide-angle X-ray diffraction (WAXD) patterns were obtained for the samples using a Bruker D8 Discover diffractometer equipped with GADDS as two-dimensional detector. Calibration of the instrument was conducted using silicon powder and silver behenate. Samples were then mounted on the sample stage, and the point-focused X-ray beam was aligned perpendicular to the sample plane. The two-dimensional diffraction patterns were recorded at room temperature in transmission mode, from which the WAXD profiles were extracted because of the isotropic characteristic of the samples.

3. Results and discussion

3.1. Temperature dependence of the ionic conductivity

Fig. 1a and b shows the temperature dependence of the ionic conductivity for all the samples in the temperature range from 27 °C to 80 °C. For the pure SN, the conductivity increases from 8.1×10^{-7} S/cm in the plastic crystal state at 43 °C to 3.4×10^{-6} S/cm in molten state at 60 °C. The standard relative uncertainty of the conductivity measurements for each temperature was less than 5%. The addition of 5% $LiClO_4$ to SN enhances the conductivity by three orders of magnitude in both solid and liquid states (at 27 °C, the conductivity is 6.6×10^{-7} S/cm for SN and 6.3×10^{-4} S/cm for SN/$LiClO_4$ 95/5 sample; at 80 °C, conductivity is 6.0×10^{-6} S/cm for SN and 8.2×10^{-3} S/cm for SN/$LiClO_4$ 95/5 sample). Note that the room temperature conductivity of the SN/$LiClO_4$ 95/5 sample (6.3×10^{-4} S/cm) is lower than that of recently reported SN/LiTFSI 95/5 sample (3.0×10^{-3} S/cm) [6], which may be due to the low capacity of TFSI anions to be electron donors. It is interesting that a larger drop of the room temperature conductivity occurs for the sample with addition of 10% PEO (PEO/SN/$LiClO_4$ 10/85/5 sample, conductivity = 2.8×10^{-4} S/cm) compared with SN/$LiClO_4$ 95/5 sample (conductivity = 6.3×10^{-4} S/cm). With a further increase of the PEO concentration from 20% to 50%, conductivity becomes higher than that of the samples with PEO concentration of 0% and 10% below the melting point. However, when the PEO concentration exceeds 70%, conductivity begins to decrease sharply with an increasing PEO concentration. For example, the room temperature conductivity of PEO/SN/$LiClO_4$ 75/20/5 sample is about 4.5×10^{-4} S/cm; while the conductivity of PEO/SN/$LiClO_4$ 95/0/5 sample (with no SN component) sharply drops to 6.3×10^{-6} S/cm. Fig. 1c summarizes the conductivity variation with PEO concentration at room temperature (27 °C). It can be seen that the room temperature conductivity first decreases for a 10% PEO concentration, but it then increases with increasing PEO concentration in the 20–50% PEO concentration range, and finally conductivity drops dramatically beyond a 70% PEO concentration. Next, we consider the evolution in material morphology accompanying these conductivity changes.

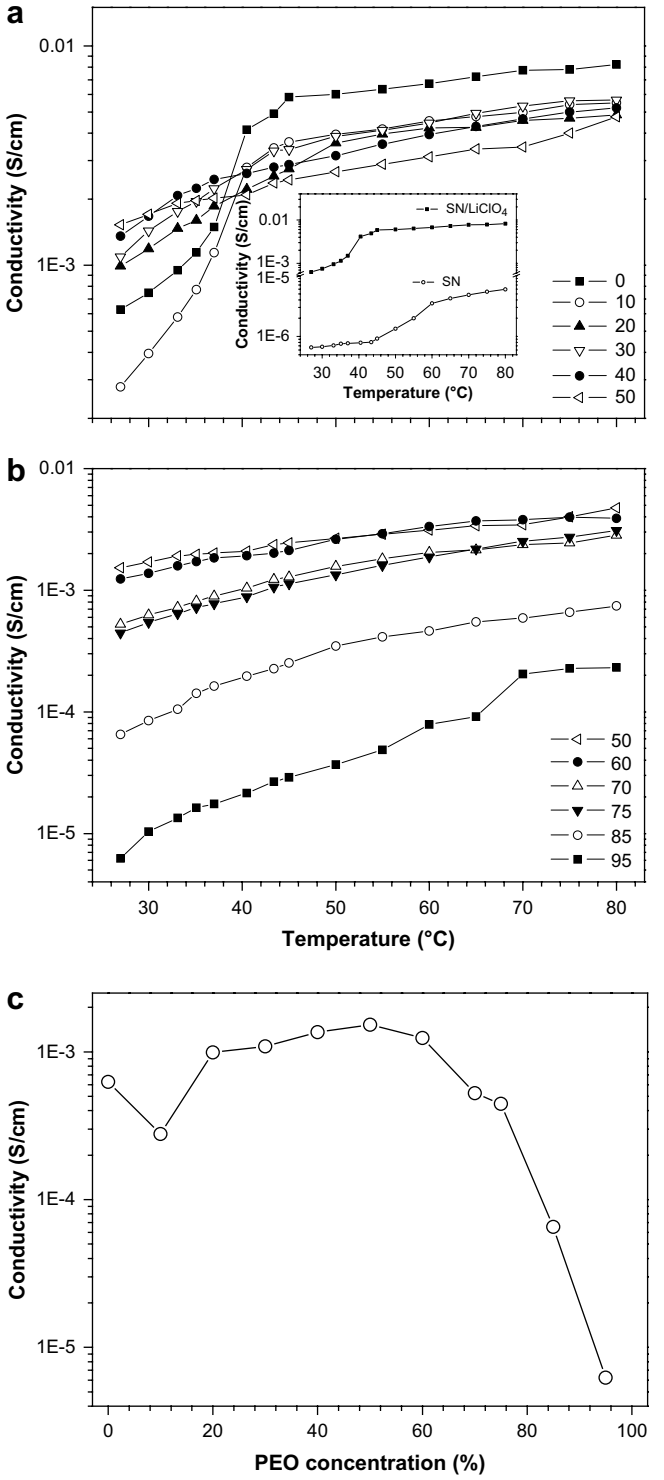

Fig. 1. Plots of conductivity versus temperature for PEO/SN/$LiClO_4$ (x/95–x/5) electrolytes where the % molar PEO concentration x varies (a) from 0% to 50% (b) from 50% to 95%. Inset in (a) compares the changes of conductivity with temperature between SN/$LiClO_4$ and SN. (c) Variation of conductivity versus PEO concentration at 27 °C. The lines connecting the data points are drawn to guide the reader's eyes. The standard relative uncertainty of conductivity for each temperature is less than 5%.

3.2. Large-scale morphologies observed by optical microscopy

Fig. 2 shows optical micrographs of the PEO/SN/$LiClO_4$ samples with increasing PEO concentrations at ambient temperature (27 °C) and provides direct insight into the conductivity variations found in

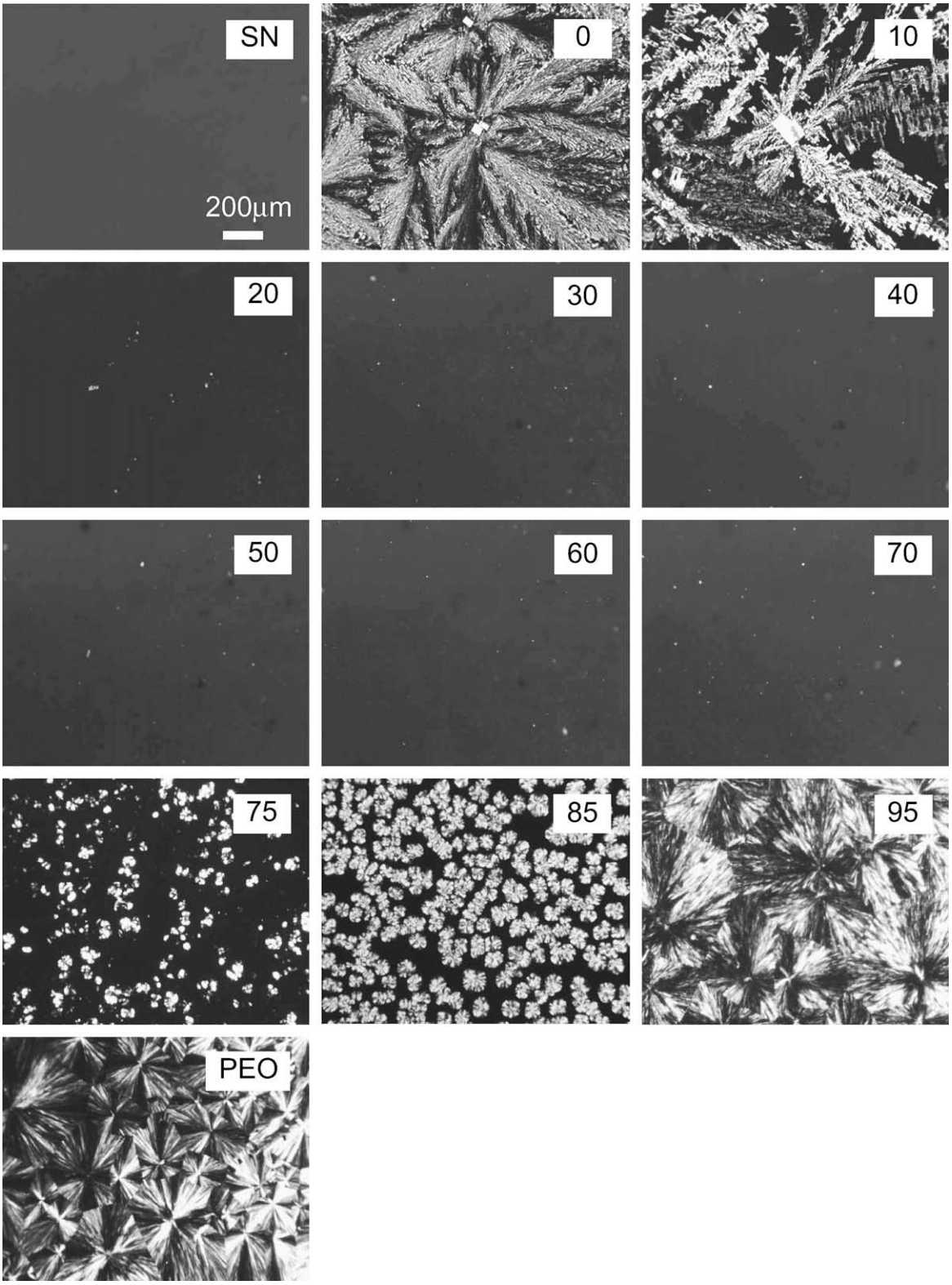

Fig. 2. Polarized optical micrographs of SN, PEO and PEO/SN/$LiClO_4$ electrolytes at room temperature. The number in each micrograph indicates the % molar PEO concentration.

the previous section. The crystallizations of PEO and SN both involve the formation of spherulites under the thermodynamic conditions of our measurements. The spherulitic morphology is easily identified by using conventional polarized optical microscopy (Fig. 2). Note that the crossed polarizer and analyzer were applied during observation. For the pure SN sample, no obvious morphological features can be observed in the microscope at a μm scale. When a small amount of $LiClO_4$ is added into the SN (SN/$LiClO_4$ 95/5 sample), spherulites form having macroscopic diameters (several mm). These are apparently SN spherulites where the

$LiClO_4$ salt serves as "impurity" that is responsible for the spherulite formation [18–21]. The nearly square structures at the centers of spherulites are interpreted to arise from cubic crystals of $LiClO_4$. With the addition of 10% PEO to the system (the PEO/SN/$LiClO_4$ 10/85/5 sample), we obtain progressively more irregular spherulites compared with the sample with no PEO, thus indicating an interference *of SN plastic crystal formation by the PEO*. This is the effect that we had hoped to see in our measurements.

When the PEO concentration became larger than 20%, we could no longer observe spherulite formation by optical microscopy. This apparent absence of spherulites persists up to a 70% PEO concentration. With a further increase of the PEO concentration to 85%, large PEO spherulites start to form with a final size of about 80 μm. (The standard relative uncertainty of the spherulite diameter measurement was less than 15%.) Evidently, SN also acts to suppress the PEO crystallization. Finally, the sample having a PEO concentration of 95% (the PEO/SN/$LiClO_4$ 95/0/5 sample) and the pure PEO sample give rise to much larger PEO spherulites that exhibit classical Maltese cross-extinction patterns under a polarizing microscope. These observations are broadly consistent with previous particular reports for these mixtures, especially in the high PEO concentration regime [16,22,23] and the pure SN regime [18] where most of the former measurements have been made.

If the conductivity variation in Fig. 1c is compared with the morphological evolution discussed above, we find that the relatively high conductivity at intermediate PEO concentrations (20–60%) near room temperature directly corresponds to the concentration range regime where both SN and PEO crystallizations are suppressed at optical scales. Although Fan et al. [13] tentatively attributed the conductivity enhancement to a low crystallinity, as judged from DSC measurements, our optical micrographs provide the first direct observation of the morphological changes responsible for the dramatic conductivity changes found in these polymer–electrolyte mixtures. To obtain more detailed information about the underlined relation between ionic conductivity and phase behaviors, DSC and WAXD measurements were performed on all of the samples.

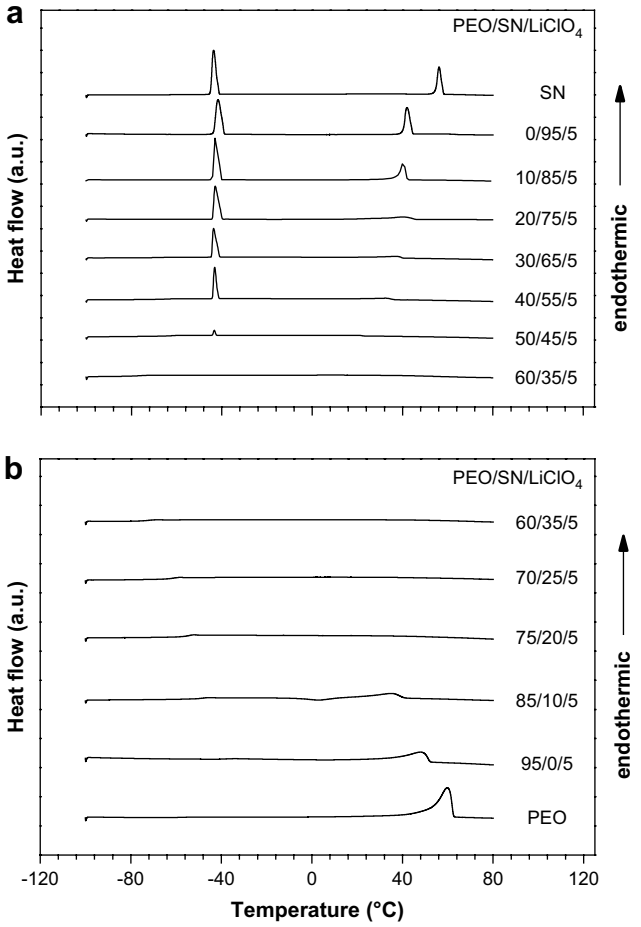

Fig. 3. DSC heat flow curves during heating scan at heating rate of 10 °C min^{-1} for SN, PEO and PEO/SN/$LiClO_4$ (x/95–x/5) electrolytes. Note that the values of the % molar PEO concentration x vary from 0% to 60% for (a) and from 60% to 95% for (b).

3.3. Thermodynamic and diffraction measurements

Heat flow curves of SN, PEO and PEO/SN/$LiClO_4$ samples were measured by DSC and the results are shown in Fig. 3a (for SN and PEO/SN/$LiClO_4$ with PEO concentration from 0% to 60%) and Fig. 3b (for PEO and PEO/SN/$LiClO_4$ with PEO concentration from 60% to 95%). From Fig. 3a, it is apparent that SN undergoes two thermodynamic transitions during the heating scan, the first peak at −43 °C indicates a solid–solid transition from the conventional crystal phase to plastic crystal phase (T_{pc}) and the second peak near 56 °C corresponds to a melting of plastic crystal phase (T_m). Slightly different phase transition peaks have been reported by different research groups, possibly due to the different experimental conditions. For example, our DSC results indicate T_{pc} of −43 °C and T_m of 56 °C, Finbak [24] reports T_{pc} of −40 °C and T_m of 58 °C, and Fan and Maier [13] report T_{pc} of −32 °C and T_m of 57 °C. The relative uncertainty of our DSC measurements for each temperature was less than 1%. In the case of SN doped with 5% $LiClO_4$ (the SN/$LiClO_4$ 95/5 sample), the first phase transition temperature (T_{pc}) shifts slightly upwards to −41 °C, while T_m is dramatically depressed to 42 °C, due to impurity effect of $LiClO_4$ on SN crystal formation [7,13]. The entropies of fusion of SN (11.9 J mol^{-1} K^{-1}) and SN/$LiClO_4$ electrolyte (12.8 J mol^{-1} K^{-1}) are within the 20.0 J mol^{-1} K^{-1} range, indicating that the second peak is due to the melting of plastic crystal phase in these two samples [4]. In addition to the changes of phase transition temperatures of the PEO/SN/$LiClO_4$ samples, the enthalpies for both thermodynamic transitions gradually decrease with increasing PEO concentration over a range from 20% to 50%, and the transition peaks could hardly be detected when the PEO concentration reached 60% (the PEO/SN/$LiClO_4$ 60/35/5 sample). With a further increase of the PEO concentration from 60% to 75% (Fig. 3b), there are *no detectable peaks* over the whole heating scan, indicating a complete disappearance of SN plastic crystal phase for these samples. Our argument about the disappearance of SN plastic crystal phase and formation of SN liquid phase for the PEO/SN/$LiClO_4$ system is consistent with that for the PEO/SN/LITFSI system by Fan and Maier [13], in which they claimed that PEO and SN somehow 'interact' with each other. The interaction between PEO and SN might be the donor–acceptor complexation (D–A interaction) between oxygen atoms (donor) in PEO chains and N≡C– groups (acceptor) in N≡C–CH_2–CH_2–C≡N molecules of SN. Furthermore, when PEO becomes the majority component in the system (with a PEO concentration above 75%), a broad peak in the high temperature region can be observed, indicating the melting of the PEO crystal phase. For the pure PEO control sample, the melting peak is found to be near 60 °C.

In order to quantify the effects of the PEO concentration on the thermal properties of the PEO/SN/$LiClO_4$ samples, we determined the transition temperatures and enthalpies of fusion of the solid–solid phase transition (T_{pc} and ΔH_{pc}) and the corresponding transition temperature and enthalpy parameters governing the SN melting process (T_m and ΔH_m). The PEO concentrations in the samples ranged from 0% (PEO/SN/$LiClO_4$ 0/95/5 sample) to 50%

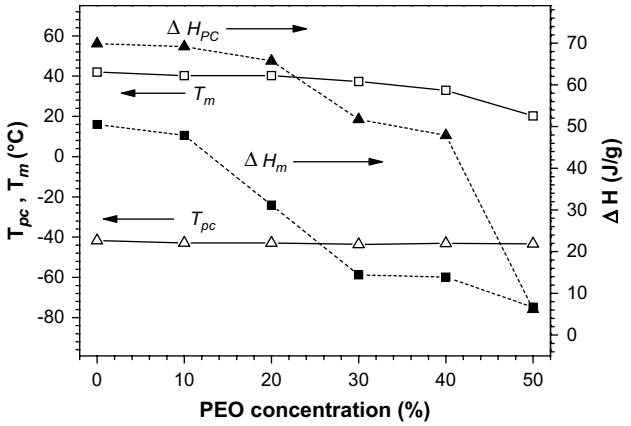

Fig. 4. Variations of phase transition temperatures (T_m and T_{pc}) and enthalpies of fusion (ΔH_{pc} and ΔH_m) as functions of PEO concentration for PEO/SN/$LiClO_4$ electrolytes. The lines connecting the data points are drawn to guide the reader's eyes. The standard relative uncertainties of the transition temperatures (T_m and T_{pc}) and enthalpies of fusion (ΔH_{pc} and ΔH_m) are less than 1%.

(PEO/SN/$LiClO_4$ 50/45/5 sample) and the corresponding data are shown in Fig. 4. Unfortunately, the faintness of the phase transition peaks for the samples having a PEO concentration above 60% does not allow for a quantitative estimate of ΔH_{pc} and ΔH_m in this high polymer concentration range.

As can be seen from Fig. 4, the addition of PEO does not significantly modify T_{pc} of the PEO/SN/$LiClO_4$ system [4]. The decrease of T_m with increasing PEO concentration is stronger than the corresponding decrease of T_{pc}. Specifically, when the PEO concentration increases from 0% to 50%, T_{pc} drops by relative amount of 4.3%, while T_m drops by as much as 52%. We also observe that the melting peak in Fig. 3a becomes smaller and broader in comparison with the solid–solid phase transition peak, and that the melting peak cannot be detected for PEO concentrations larger than 20%. Furthermore, it is apparent from Fig. 4 that the enthalpies of fusion of both the solid–solid thermodynamic transition and the melting transition both drop sharply for the sample having a PEO concentration near 20%. It should be mentioned that the DSC curves during cooling were obtained for examining the potential hysteresis and the reproducibility of phase transition temperature determinations. Since the DSC results during cooling basically support the data during heating, they are not shown in this paper.

While there is evidence for an apparent SN solid–solid phase transition from the DSC heat flow curves in some cases above a 20% PEO concentration, we could not observe spherulitic SN plastic crystal structures by polarized optical microscopy at ambient temperature in the concentrated PEO regime. Evidently, the crystals must be smaller than the scales detectable by our optical measurements. Considering the significant drop of ΔH_m from the DSC measurements, and the absence of spherulites from the polarized optical microscope images for PEO/SN/$LiClO_4$ samples with PEO concentration of 20% or greater, it is at least clear that the fraction of SN plastic crystalline material is much reduced by the PEO additive. This qualitative result is enough to explain the relative enhancement in ionic conductivity of the polymer–electrolyte at room temperature relative to the material without the polymer additive.

From the DSC and optical microscopy results, we infer that there is a gradual evolution in crystal morphology with increasing PEO concentration from a well-ordered SN plastic crystal phase to a largely amorphous structure containing small inclusions of the SN plastic crystal and PEO crystals too fine to be observed by optical microscopy. Apparently, the interference of the crystallization of one crystallizing component of the mixture (SN) by the presence of another species (PEO) gives rise to net suppression of large-scale crystal growth. We next consider diffraction measurements to gain insight into the fine scale structure of these 'frustrated' materials that is inaccessible by optical microscopy.

We performed wide-angle X-ray diffraction (WAXD) measurements for all the samples in the angular range $7.5^\circ < 2\theta < 37.5^\circ$. Our observations are summarized in Fig. 5a (for SN, $LiClO_4$ and PEO/SN/$LiClO_4$ with PEO concentration from 0% to 50%) and Fig. 5b (for PEO and PEO/SN/$LiClO_4$ with PEO concentration from 50% to 95%). From Fig. 5a, we see that the pure SN sample at room temperature exhibits two characteristic peaks around $2\theta = 19.8^\circ$ and 28.1°, while $LiClO_4$ shows one peak around $2\theta = 24.6^\circ$. The PEO/SN/$LiClO_4$ 0/95/5 and 10/85/5 samples show a faint peak at $2\theta = 28.1^\circ$ and three other peaks near $2\theta = 22.0^\circ$, 23.3° and 24.8° that have been attributed to the interaction between SN and $LiClO_4$ [25]. Upon increasing the PEO concentration from 20% to 40%, the peaks around $2\theta = 22.0^\circ$, 23.3° and 24.8° simply disappear, the SN related peak around $2\theta = 19.8^\circ$ becomes faint, and the other SN peak around $2\theta = 28.1^\circ$ gradually disappears. [The SN nitrile group has a lower Gutmann donor number [6] than the oxygen of PEO so that SN has less of a capacity to solvate Li cations than PEO. Thus, it is possible for PEO to compete with SN in these samples (PEO/SN/$LiClO_4$ 20/75/5, 30/65/5 and 40/55/5) in its ability to coordinate

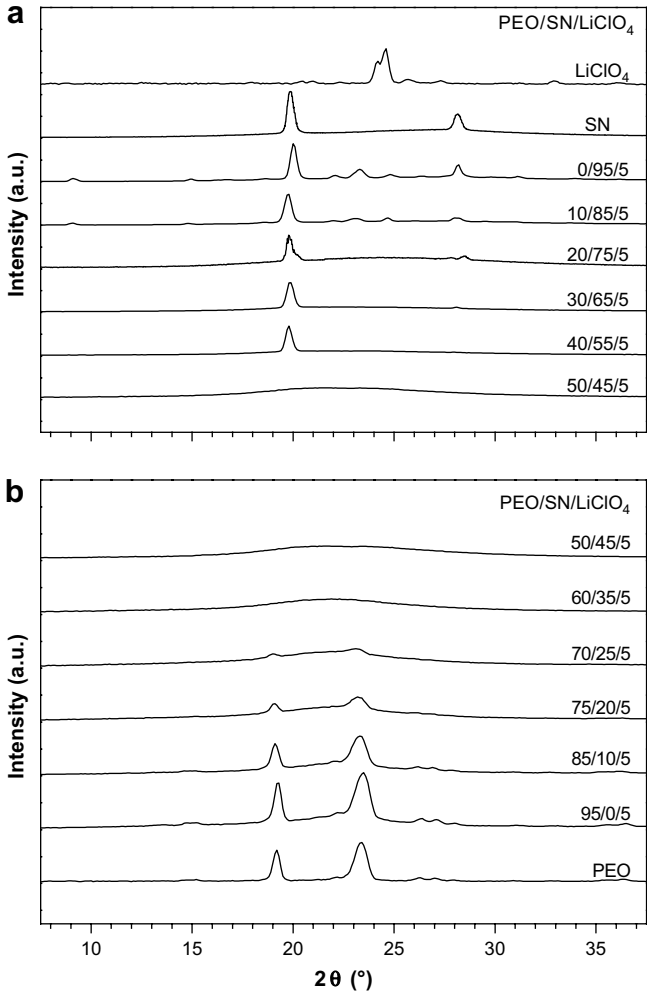

Fig. 5. Wide-angle X-ray diffraction (WAXD) profiles for SN, $LiClO_4$, PEO and PEO/SN/$LiClO_4$ (x/95–x/5) electrolytes. Note that the values of the % molar PEO concentration x vary from 0% to 50% for (a) and from 50% to 95% for (b).

with the dopant $LiClO_4$, accounting for the peaks near the positions: $2\theta = 22.0^\circ$, 23.2° and 24.8°.] We then see that the addition of PEO inhibits the formation of the SN plastic crystal phase, even at molecular scales, as evidenced by the WAXD profiles showing that the peak intensities of the SN plastic crystal phase decrease with increasing PEO concentration. Fig. 5b indicates that the samples with a PEO concentration in the range between 50% and 70% (PEO/SN/$LiClO_4$ 50/45/5, 60/25/5 and 70/20/5) exhibit WAXD profiles without any distinct peaks, indicating the presence of a *completely homogeneous amorphous material*. This is consistent with the DSC measurements and large-scale optical microscopy observations described earlier. For the polymer–electrolyte mixtures with a high PEO concentration (in the range between 75% and 95%) and the pure PEO sample, the WAXD profiles show two peaks (Fig. 5b) at around $2\theta = 19.2^\circ$ and 23.3° and the intensities of these peaks increase with the PEO concentration, signaling an increasing PEO crystallinity. The essential disappearance of both the characteristic DSC and WAXD peaks corresponding to the SN plastic crystal phase for PEO concentrations in the range from 20% to 60% provides confirmation of optical microscopy observations indicating that crystallization in these materials has been largely suppressed in an intermediate PEO concentration range (from 20% to 60%). It might be considered that the local ordering of one species creates a quenched disorder that inhibits ordering of the other species. The mechanism here is sensitive to the formation of glasses where local ordering incommensurate with the final ordered state inhibits the development of the proper crystal. Note the effect is quite general and the polymeric nature of the medium is irrelevant. However, further studies and confirmation are worth in the future.

3.4. Temperature dependence of ionic conductivity

Our examination of the SN electrolyte materials having an intermediate PEO concentration range (20–60%) indicates that these are 'glassy' materials, i.e., the materials for which crystallization is frustrated by some type of disorder that is either of an intrinsic nature (derived from the fluid molecular structure) or extrinsic nature (derived from heterogeneities introduced into the fluid or at its boundaries). Correspondingly, it is natural to consider whether the conductivity of these complex materials conforms to the standard phenomenology of glass-forming liquids. We then compare the temperature dependence of conductivity for our PEO/SN/$LiClO_4$ mixtures in the intermediate PEO concentration range to the Vogel–Fulcher–Tamman (VFT) relation [26]. The VFT relation describes the temperature dependence of structural relaxation in an extraordinarily large number of glassy materials [27–30] and the particular transport property, the conductivity σ is defined by the simple VFT relation,

$$\sigma = A \exp[-BT_0/(T - T_0)], \quad B \text{ is dimensionless} \tag{1}$$

where A and B are parameters and T_0 is a temperature where σ formally extrapolates to zero. (Although this relationship is mainly viewed as phenomenological, it has recently been derived for structural relaxation in polymeric glass-forming liquids based on the entropy theory of glass-formation [31].) Fig. 6a shows a fit of the VFT relation to a 'glassy' mixture of PEO with the plastic crystal electrolyte for a PEO concentration of 40% in the middle of the frustrated crystallization regime. The standard relative uncertainty of conductivity for each temperature was less than 5%. It can be seen that the fit to the VFT equation is quite satisfactory, confirming the glassy nature of the material. Fitting our conductivity data for different PEO concentrations in this intermediate PEO concentration range regime indicates a systematic variation in the 'fragility' parameter B. [Fluids with relatively larger B values are conventionally termed 'strong' fluids [26] since a larger value of B implies a weaker deviation from an Arrhenius temperature dependence. Fluids with a smaller value of B are correspondingly said to be relatively 'fragile', regardless of the physical origin of this behavior.] Fig. 6b indicates that B increases with increasing PEO concentration. The result indicates that ionic mobility, along with PEO segmental motions, becomes reduced with an increasing PEO concentration. Note that fits of the conductivity data to the VFT relation are no longer acceptable for PEO concentrations far outside of the intermediate PEO concentration range regime (from 20% to 60%) where the polymer–electrolyte material can reasonably described as predominantly 'amorphous'.

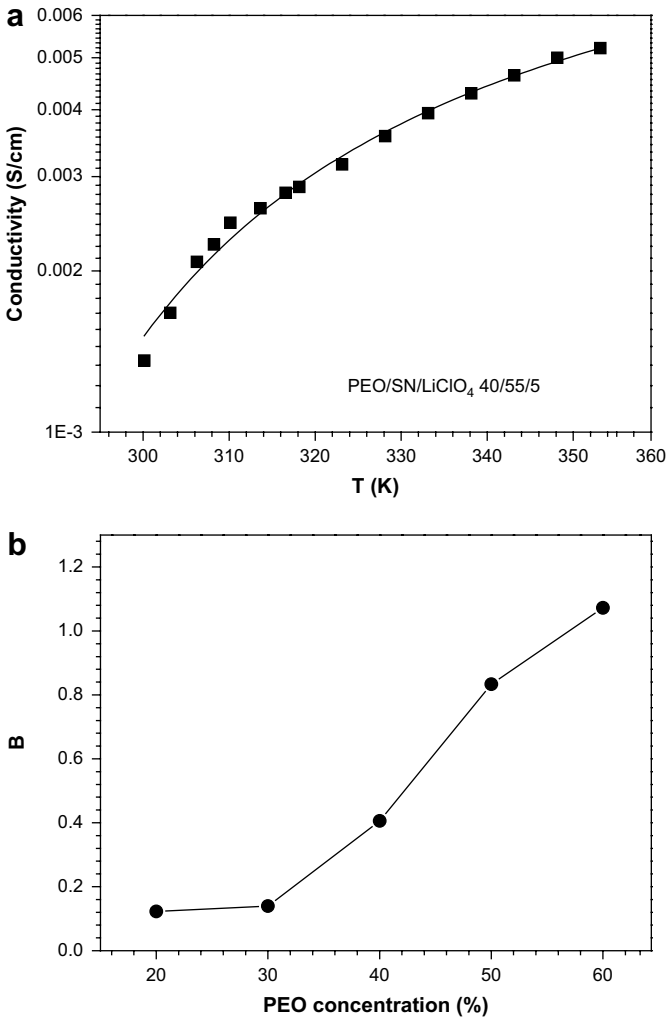

Fig. 6. Typical VFT plot of conductivity versus temperature for the PEO/SN/$LiClO_4$ 40/55/5 sample. Solid curve shows a fit of the data to the VFT equation (a); and B as a function of PEO concentration for PEO/SN/$LiClO_4$ (x/95–x/5) electrolytes, where the % molar PEO concentration x varies from 20% to 60%. The line connecting B data points is drawn to guide the reader's eyes (b). The standard relative uncertainty of conductivity for each temperature is less than 5%. The correlation coefficient in the fit to the VFT equation is larger than 0.965.

4. Conclusions

We implement a novel method of stabilizing plastic crystal electrolytes that relies on the *competition* between the crystallization of the plastic crystal electrolyte mixture and the polymeric additive. The beneficial effect of this mixing is optimized at intermediate PEO concentrations where large-scale crystallizations of

the plastic crystal and PEO are *both* effectively inhibited. The polymer additive has the added benefit of enhancing the mechanical properties of these plastic crystal electrolyte materials.

The relationship between ionic conductivity and morphology, as well as phase transitions and thermal properties of PEO/SN/$LiClO_4$ electrolytes, was investigated by polarized optical microscopy, differential scanning calorimetry, and wide-angle X-ray diffraction. We find that the binary succinonitrile/lithium perchlorate (SN/$LiClO_4$) plastic crystal electrolyte shows room temperature ionic conductivity of 6.3×10^{-4} S/cm with a SN spherulitic morphology. With the addition of a low concentration of PEO, we still obtain SN spherulites, but these structures become progressively coarser in structure with an increasing PEO concentration until SN spherulite formation is unobservable optically beyond a 20% (molar concentration) of PEO. (While spherulites were not observable optically, WAXD and DSC measurements suggest that this type of crystallization exists at smaller scales.) Increasing the PEO concentration further to 70% leads to a high PEO concentration regime where large-scale PEO spherulites become prevalent. The intermediate PEO concentration range regime (20–60%), where large-scale SN and PEO crystallization processes are *both* relatively inhibited, proves to be most interesting from the standpoint of battery applications. Specifically, conductivity measurements on these glassy materials show that the relatively high conductivity of the pure fluids at high temperatures can be largely preserved near room temperature through the addition of PEO, in contrast to the crystalline materials formed at low and high PEO concentrations. These observations demonstrate that our method of suppressing crystallization is effective in creating highly conductive solid ionic materials that are promising for battery applications.

Evidently, the polymer–electrolyte mixtures at intermediate PEO concentrations are glassy fluids of predominantly amorphous structure and conductivity of these complex mixtures also exhibits the characteristic temperature dependence of glass-forming liquids. Crystallization of the SN is frustrated by the polymer additive and the crystallization of PEO is correspondingly frustrated by the presence of the SN electrolyte. Increasing the PEO concentration leads to a point where the PEO begins to crystallize appreciably, however. The more restricted ionic mobility caused by the PEO crystallinity then leads to a dramatic decrease of ionic conductivity. On the positive side, this increased crystallinity enhances some mechanical properties such as modulus, but it diminishes other properties such as the material toughness.

Acknowledgements

ZG Wang thanks financial support from National Science Foundation of China with grant number 10590355 for the Key Project on Evolution of Structure and Morphology during Polymer Processing. We also thank Prof. Shibi Fang in our institute for his helpful suggestions and for offering us the use of an AC impedance device, and Prof. Jerold Schultz of the University of Delaware for his comments on an earlier version of the manuscript.

Appendix. Basic rheological characterization of PEO–SN electrolyte mixtures

Fig. A1(a) and (b) indicates the storage G' and loss G'' components of the frequency dependent shear modulus and their ratio $\tan\delta$ as functions of frequency ω where the measurements were performed at 30 °C. The polydispersity of the PEO sample was measured by gel permeation chromatography to equal, $M_w/M_n = 1.8$ and the PEO concentration equaled 50% for PEO/SN/LiClO4 50/45/5 and 65% for PEO/SN/LiClO4 65/30/5.

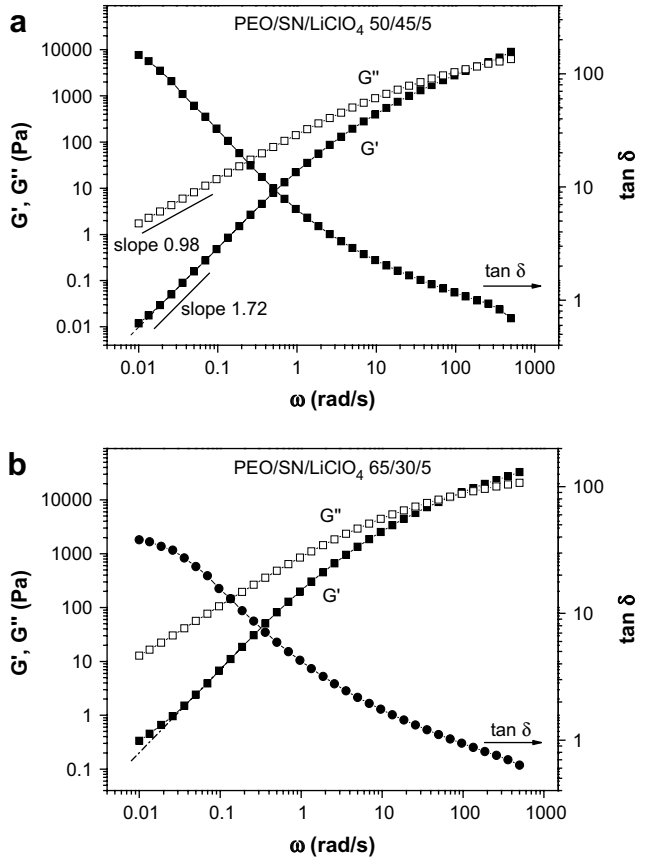

Fig. A1. Variations of G', G'' and $\tan\delta$ with frequency ω at 30 °C for the samples with PEO concentration of 50% (a) and 65% (b). The lines connecting the data points are drawn to guide the reader's eyes. The standard relative uncertainties for G', G'' and $\tan\delta$ are less than 1%.

According to Winter and Francois [32,33], the frequency independence of $\tan\delta$ in the vicinity of gel point is a direct characteristic for both chemical and physical gels, and hence provides a useful criterion for gel formation. At the critical gel point, rheological features, for example, the dynamic moduli G^*, loss tangent $\tan\delta$, and viscosity η^* exhibit dramatic changes that serve to precisely locate the gelation transition. Specifically, these materials exhibit the scaling laws $G' \sim \omega^2$ and $G'' \sim \omega^1$ in the terminal region for homogeneous fluids, while G' and G'' power laws vary in the oscillatory frequency ω (i.e., $G' \sim G'' \sim \omega^n$) as the amorphous solid sate of the gel first emerges [34]. From Fig. A1(a), it is apparent that for the sample having a PEO concentration of 50%, the corresponding slopes of G' and G'' in the low frequency regime are 1.72 and 0.98, respectively, which means the sample is still fluid, albeit viscoelastic in nature. When the PEO concentration increases to 65%, however, a short plateau region of $\tan\delta$ develops at low frequencies, suggesting the emergence of gel-like rheological behavior.

References

[1] Abu-Lebdeh Y, Alarco PJ, Armand M. Angewandte Chemie International Edition 2003;42:4499.
[2] Yoshizawa-Fujita M, Fujita K, Forsyth M, MacFarlane DR. Electrochemistry Communications 2007;9:1202.
[3] Pas SJ, Efthimiadis J, Pringle JM, Forsyth M, MacFarlane DR. Journal of Materials Chemistry 2004;14:2603–5.
[4] MacFarlane DR, Huang JH, Forsyth M. Nature 1999;402:792.
[5] Sun J, MacFarlane DR, Forsyth M. Solid State Ionics 2002;148:145.
[6] Alarco PJ, Abu-Lebdeh Y, Abouimrane A, Armand M. Nature Materials 2004;3:476.
[7] Long S, MacFarlane DR, Forsyth M. Solid State Ionics 2003;161:105.

[8] Volel M, Alarco PJ, Abu-Lebdeh Y, Armand M. Physical Chemistry Chemical Physics 2004;5:1027.
[9] Chu PP, Jen HP, Lo FR, Lang CL. Macromolecules 1999;32:4738.
[10] Volel M, Armand M, Gorecki W. Macromolecules 2004;37:8373.
[11] He XM, Pu WH, Wang L, Jiang CY, Wan CR. Progress in Chemistry 2006;18:24.
[12] Abu-Lebdeh Y, Abouimrane A, Alarco PJ, Hammami A, Ionescu-Vasii L, Armand M. Electrochemistry Communications 2004;6:432.
[13] Fan LZ, Maier J. Electrochemistry Communications 2006;8:1753.
[14] Fan LZ, Hu YS, Bhattacharyya AJ, Maier J. Advanced Functional Materials 2007;17:2800.
[15] Certain equipment, instruments, or materials are identified in this paper in order to adequately specify the experimental details. Such identification does not imply recommendation by the NIST, nor does it imply that the materials are necessarily the best available for the purpose. The obsolete term 'molecular weight' is replaced by the equivalent, but more accurate term, relative molecular mass [4: ISO 31-8].
[16] Xi JY, Qiu XP, Zheng SX, Tang XZ. Polymer 2005;46:5702.
[17] Sumathipala HH, Hassoun J, Panero S, Scrosati B. Ionics 2007;13:281.
[18] Sekhar JA, Trivedi R. Materials Science and Engineering A – Structural Materials Properties Microstructure and Processing 1991;147:9.
[19] Granasy L, Pusztai T, Warren JA, Douglas JF, Borzsonyi T, Ferreiro V. Nature Materials 2003;2:92.
[20] Granasy L, Pusztai T, Borzsonyi T, Warren JA, Douglas JF. Nature Materials 2004;3:645.
[21] Granasy L, Pusztai T, Tegze G, Warren JA, Douglas JF. Physical Review E 2005:72.
[22] Xi JY, Qiu XP, Wang JS, Bai YX, Zhu WT, Chen LQ. Journal of Power Sources 2006;158:627.
[23] Choi BK. Solid State Ionics 2004;168:123.
[24] Sherwood JN. The plastically crystalline state: orientationally disordered crystals. London: Wiley; 1979.
[25] Abouimrane A, Whitfield PS, Niketic S, Davidson IJ. Journal of Power Sources 2007;174:883.
[26] Angell CA. Science 2008;319:582.
[27] Gray FM. Polymer electrolytes. Cambridge: The Royal Society of Chemistry; 1997.
[28] Carvalho LM, Guegan P, Cheradame H, Gomes AS. European Polymer Journal 2000;36:401.
[29] Ahmad S, Saxena TK, Ahmad S, Agnihotry SA. Journal of Power Sources 2006;159:205.
[30] Kumar SK, Douglas JF. Physical Review Letters 2001;87:188301.
[31] Dudowicz J, Freed KF, Douglas JF. Advances in Chemical Physics 2008;137:125.
[32] Winter HH, Francois C. Journal of Rheology 1986;30:367.
[33] Francois C, Winter HH. Journal of Rheology 1987;31:683.
[34] Goldenfeld N, Goldbart P. Physical Review A 1992;45:R5343.